CAMS Service Evolution

D3.2 Report on satellite lidar, ceilometer and AOD assimilation

Due date of deliverable	30 November 2025
Submission date	23 December 2025
File Name	CAMEO-D3-2-V1.1
Work Package /Task	WP 3 / Task 3.2
Organisation Responsible of Deliverable	Météo-France
Author name(s)	Vincent Guidard, Mickaël Bacles,Nicolas Frebourg, Guillaume Monteil, Andreas Uppstu, Jeronimo Escribano
Revision number	V1.1
Status	Issued
Dissemination Level	Public

Funded by the European Union

The CAMEO project (grant agreement No 101082125) is funded by the European Union.
Views and opinions expressed are however those of the author(s) only and do not necessarily reflect those of the European Union or the Commission. Neither the European Union nor the granting authority can be held responsible for them.

1 Executive Summary

Aerosols are of particular importance as they have a large impact both on air quality, for which the forecast of particulate matter concentration at surface are used, and on many tropospheric aspects like effect on radiation reaching the surface and cloud interactions.

In order to improve forecasts made at regional scale over Europe, the assimilation of observations relevant for aerosols has been studied in the task 3.2 of the CAMEO project.

The first type of instrument that has been selected is the remote sensing of aerosols from the ground using lidars and ceilometers from the e-profile European network. 4 types of instruments sensing at different wavelengths provide information on the vertical profile of aerosols through their attenuated backscatter signal. Such data has been assimilated in the regional domain of the chemistry-transport model MOCAGE. A cautious preprocessing has been applied to remove any spurious signal from clouds, rain of noise. The observation errors have been refined using the so-called Desroziers diagnostic. Improvements have been found on the quality of the PM10 forecasts compared against in situ EEA measurements. This impact lasts during the first 36 to 48 h of forecast range.

Although the e-profile observations have a good potential positive impact on forecasts, their assimilation requires an advanced assimilation system so that it can fit in an operational timing in near real time.

The other type of observation considered in this study is the space-borne measurements of Aerosol Optical Depth (AODs). Many satellite platforms embark visible – near infrared instruments that have the capacity to provide AODs. The VIIRS instrument has been chosen, as it is onboard operational satellites of the US JPSS series. Three different models (MOCAGE, MONARCH and SILAM) have evaluated the impact of assimilating VIIRS AODs over Europe. The conclusions highlight a rather neutral impact on surface particulate matter forecasts. Contrary to e-profile data, satellite AODs do not provide a detailed vertical information. Moreover, polar-orbiting satellites only overpass Europe a few hours a day.

More work is needed to gain from satellite AODs. One possible way forward would be to consider AODs from geostationary instruments like FCI and/or explore AODs from specific species, like dust AODs (from IRS, e.g.).

Table of Contents

2 Introduction

2.1 Background

Monitoring the composition of the atmosphere is a key objective of the European Union's flagship Space programme Copernicus, with the Copernicus Atmosphere Monitoring Service (CAMS) providing free and continuous data and information on atmospheric composition.

The CAMS Service Evolution (CAMEO) project will enhance the quality and efficiency of the CAMS service and help CAMS to better respond to policy needs such as air pollution and greenhouse gases monitoring, the fulfilment of sustainable development goals, and sustainable and clean energy.

CAMEO will help prepare CAMS for the uptake of forthcoming satellite data, including Sentinel-4, -5 and 3MI, and advance the aerosol and trace gas data assimilation methods and inversion capacity of the global and regional CAMS production systems.

CAMEO will develop methods to provide uncertainty information about CAMS products, in particular for emissions, policy, solar radiation and deposition products in response to prominent requests from current CAMS users.

CAMEO will contribute to the medium- to long-term evolution of the CAMS production systems and products.

The transfer of developments from CAMEO into subsequent improvements of CAMS operational service elements is a main driver for the project and is the main pathway to impact for CAMEO.

The CAMEO consortium, led by ECMWF, the entity entrusted to operate CAMS, includes several CAMS partners thus allowing CAMEO developments to be carried out directly within the CAMS production systems and facilitating the transition of CAMEO results to future upgrades of the CAMS service.

This will maximise the impact and outcomes of CAMEO as it can make full use of the existing CAMS infrastructure for data sharing, data delivery and communication, thus supporting policymakers, business and citizens with enhanced atmospheric environmental information.

2.2 Scope of this deliverable

2.2.1 Objectives of this deliverable

This deliverable aims at providing a comprehensive overview of the results obtained in both tasks 3.2.1 and 3.2.2 of the workpackage 3 of CAMEO

2.2.2 Work performed in this deliverable

In this deliverable the work as planned in the Description of Action (WP3, task 3.2) was performed :

• Task 3.2.1: Improve the vertical description of aerosols. The characterisation of aerosols' vertical profiles is still hardly seen from satellites, except for spaceborne lidars. The E-profile programme of Eumetnet provides backscatter profiles from ground-based lidars and ceilometers with a good density over Europe (over land surfaces). We propose to review the various sensors available in the E-profile network and select which ones should be assimilated first. Then the preprocessing of the data will be examined to decide how to aggregate them before assimilation. Finally, assimilation trials will be conducted.

• Task3.2.2 Potential benefits of satellite AOD assimilation. In addition to ground-based data, satellite AOD measurements (total) will be assimilated to improve coverage over oceans, using the data from VIIRS.

2.2.3 Deviations and counter measures

No deviations have been encountered.

2.2.4 CAMEO Project Partners:

ECMWF	EUROPEAN CENTRE FOR MEDIUM-RANGE WEATHER FORECASTS
Met Norway	METEOROLOGISK INSTITUTT
BSC	BARCELONA SUPERCOMPUTING CENTER-CENTRO NACIONAL DE SUPERCOMPUTACION
KNMI	KONINKLIJK NEDERLANDS METEOROLOGISCH INSTITUUT-KNMi
SMHI	SVERIGES METEOROLOGISKA OCH HYDROLOGISKA INSTITUT
BIRA-IASB	INSTITUT ROYAL D'AERONOMIE SPATIALEDE BELGIQUE
HYGEOS	HYGEOS SARL
FMI	ILMATIETEEN LAITOS
DLR	DEUTSCHES ZENTRUM FUR LUFT - UND RAUMFAHRT EV
ARMINES	ASSOCIATION POUR LA RECHERCHE ET LE DEVELOPPEMENT DES METHODES ET PROCESSUS INDUSTRIELS
CNRS	CENTRE NATIONAL DE LA RECHERCHE SCIENTIFIQUE CNRS
GRASP-SAS	GENERALIZED RETRIEVAL OF ATMOSPHERE AND SURFACE PROPERTIES EN ABREGE GRASP
CU	UNIVERZITA KARLOVA
CEA	COMMISSARIAT A L ENERGIE ATOMIQUE ET AUX ENERGIES ALTERNATIVES
MF	METEO-FRANCE
TNO	NEDERLANDSE ORGANISATIE VOOR TOEGEPAST NATUURWETENSCHAPPELIJK ONDERZOEK TNO
INERIS	INSTITUT NATIONAL DE L ENVIRONNEMENT INDUSTRIEL ET DES RISQUES - INERIS
IOS-PIB	INSTYTUT OCHRONY SRODOWISKA - PANSTWOWY INSTYTUT BADAWCZY
FZJ	FORSCHUNGSZENTRUM JULICH GMBH

AU	AARHUS UNIVERSITET
ENEA	AGENZIA NAZIONALE PER LE NUOVE TECNOLOGIE, L'ENERGIA E LO SVILUPPO ECONOMICO SOSTENIBILE

3 Assimilation of e-profile observations

3.1 Description of the sensors and observations

E-profile is a programme within EUMETNET (https://eumetnet.eu/) which gathers 33 countries. E-profile encompasses activities with 3 means of measurements from the ground: wind profilers, microwave radiometers and aerosol profilers. We will refer the measurements of aerosol profilers within this programme as e-profile data hereafter.

At the time of the beginning of the present study, 4 types of instruments were available in the e-profile network:

- CL31: ceilometers at 900 nm wavelength
- CL51: ceilometers at 900 nm wavelength
- CHM15k: ceilometers at 1064 nm wavelength
- miniMPL: lidars at 532 nm wavelength

The network is described in Figure 1.

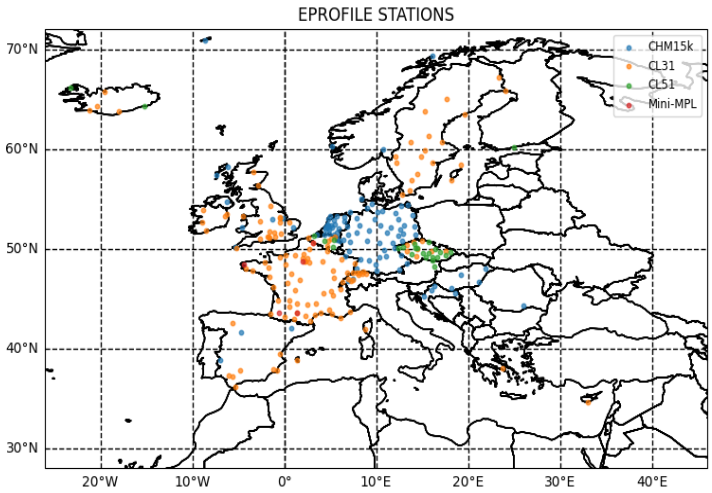

Figure 1: Location of e-profile stations for each of the sensor types (miniMPL, CHM15K, CL31 and CL51.

Within EUMETNET activities, the UK MetOffice collects the data from the whole e-profile network for aerosols and disseminates the observations in the BUFR format on the WMO Information System (WIS, formerly known as GTS) in near real time. At Météo-France, this data flow is stored in real time for operational purposes and is used in this study.

3.2 Preprocessing of the data

The preprocessing consists of a truncation of the altitude range, a cloud mask, precipitation mask, fog mask, and noise mask. It also includes the vertical interpolation onto MOCAGE's grid and a check between the altitude of the station used in MOCAGE and its actual altitude. Figure 2 recaps the different steps that are fully described below.

Altitude range. The vertical ranges provided by EUMETNET mainly reflect the instruments' limitations for cloud-base detection. For the much weaker and, potentially, noisier aerosol signal, a more conservative vertical range is adopted, depending on the instrument:

- CL31: 0–3 km
- CL51: 0–5.3 km
- CHM15k: 0–7.5 km
- miniMPL: 0.25–15 km

All data outside these ranges are masked out.

Cloud mask. Even though backscattering from clouds is generally stronger than that of aerosol plumes, the signal strengths of clouds and aerosols can significantly overlap. Therefore, clouds and aerosols cannot be reliably discriminated based on the strength of the backscattered power. However, the standard deviation of the attenuated backscatter coefficient, std(β_{att}), has been found to be an effective discriminator. More specifically, an observation of β_{att} at altitude z_l and time step t_i is regarded as a cloud, if

std[$\beta_{att}(t_i, z_l)$] > Threshold,

The threshold is taken to be 10^{-6} $m^{-1}sr^{-1}$ for CHM15k instruments, and 1.5 10^{-6} $m^{-1}sr^{-1}$ for all other instruments. Several thresholds have been tested for each instrument to determine the best value for detecting clouds without masking aerosols.

To verify the validity of our results, we compared observations marked as clouds with satellite images. We also tested these thresholds in cases of desert dust episodes. Our results showed that using a threshold that is too low leads to an overestimation of clouds, which can mask aerosols. On the contrary, a threshold that is too high can result in the retention of a large number of observations that are in reality clouds.

Precipitation mask. At each time step t_i the number of cloud layers is determined up to a maximum of three layers. If there are cloud-free model layers between two cloudy layers, and if the altitude difference between the lower and the upper cloud layer is ≥ 35 m, then the upper layer is counted as a new cloud layer. For each cloud with base altitude z_c ≥ 1 km, one considers the quantity

$$\overline{\beta}_{\mathrm{att}}(t_i, z_{\min}, z_{\max}) = \underset{z_{\min} \le z \le z_{\max}}{\mathrm{mean}} [\beta_{\mathrm{att}}(t_i, z)]$$

The precipitation mask is based on evaluating this quantity by taking the mean over all altitudes between z_{min} = z_c-1 km and z_{max} = z_c-0.5 km.

If $\overline{\beta}_{\mathrm{att}}(t_i, z_c - 1\,\mathrm{km}, z_c - 0.5\,\mathrm{km}) > 2.5\mathrm{e}-6\,\mathrm{m}^{-1}\mathrm{sr}^{-1}$, then all data at time step t_i below the cloud base z_c are masked out as precipitation.

Fog mask. Data are masked out as fog if the altitude is below 250 m, and if any of the following two conditions is satisfied:

$\beta_{att}(t_i, 0, 250\ m) > 2.5\ 10^{-6}\ m^{-1}sr^{-1}$

$\beta_{att}(t_i, 0, 250\ m) > 2\beta_{att}(t_i, 250\ m, 500\ m)$

Noise mask. Data points are masked out as noise if the following criterion is satisfied:

mean[$\beta_{att}[(t_i, z_l)]$ / std[$\beta_{att}[(t_i, z_l)]$ < 3.

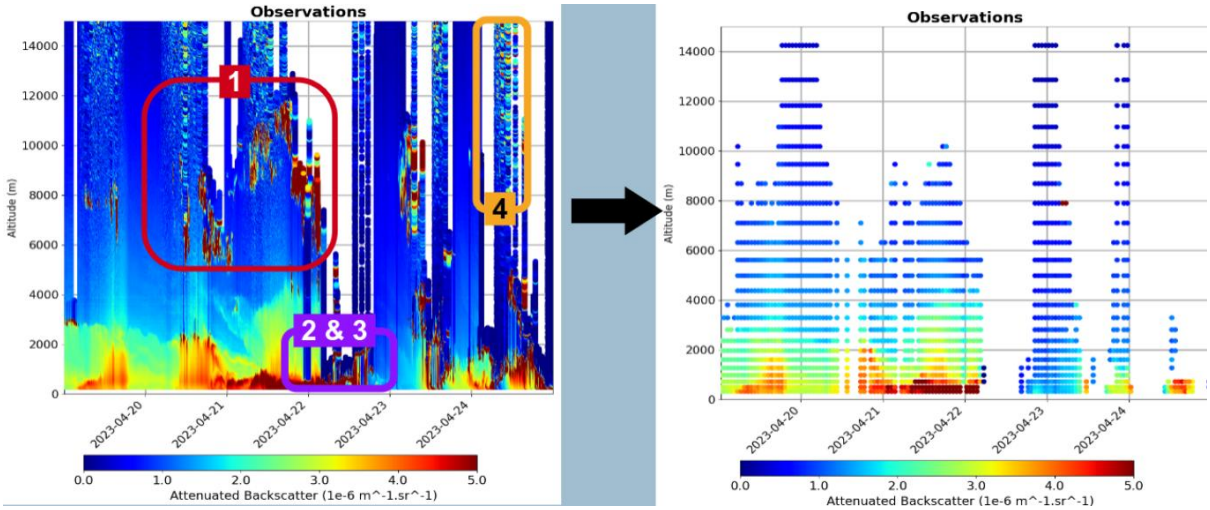

Figure 2: Illustration of the different steps in e-profile data preprocessing before their assimilation in MOCAGE. 1 Remove clouds. 2 Remove rain. 3 Remove fog. 4 Remove noisy data. 5 Observation averaging (1 observation per hour and per MOCAGE level).

3.3 Impact of assimilating e-profile observations

3.3.1 Description of MOCAGE assimilation system

MOCAGE is a three-dimensional Chemistry Transport model developed, maintained and enriched at the Centre National de Recherches Météorologiques (CNRM) at Météo-France since 2000 (e.g. Guth et al, 2016). It is used for operational and research applications on two geographical configurations: global and regional. It has notably been used for several studies aimed at assessing the impact of climate change on atmospheric chemistry, on the transport of trace gases in the troposphere, as well as on coupled meteorology-atmospheric composition assimilation for the improvement of Numerical Weather Prediction (NWP). Many efforts have been made to use MOCAGE to study the exchanges taking place between the troposphere and the stratosphere using data assimilation (), or to extend the representation of aerosols in the model simulations thanks to the assimilation of AODs (e.g. El Amraoui et al, 2022). The model is also a valuable resource for air quality monitoring and forecasting on the French Prev'Air platform and on Europe within the framework of the CAMS project (Colette et al, 2025).

The domain used for the CAMS regional service has a horizontal grid of 0.1 degree and 60 vertical levels. The assimilation system is an hourly 3D-Var assimilation over the same geographical grid as the forecast model.

3.3.2 Observation errors

In the assimilation process, an accurate definition of observation errors is needed. The R matrix represents the observation error covariances. We assume that there is no horizontal correlation, so we only represent vertical covariances.

In a first attempt, no vertical correlation is assumed and the standard deviation of the observation errors is assumed to be a percentage of the actual ATB observation (25% is used).

In Numerical Weather Prediction (NWP), a common method used to estimate the observation error covariances is the so-called Desroziers' diagnostic (Desroziers et al 2005). This method

relies on both innovations (observation minus first-guess d^o_b) and residuals (observation minus analysis d^o_a) :

Rdiagnosed = E(d^o_b $d^o_a{}^T$) where E stands for the mathematical expectation.

We have computed such a diagnostic, gathering all observations from each type of sensors. The results are shown in Figure 3.

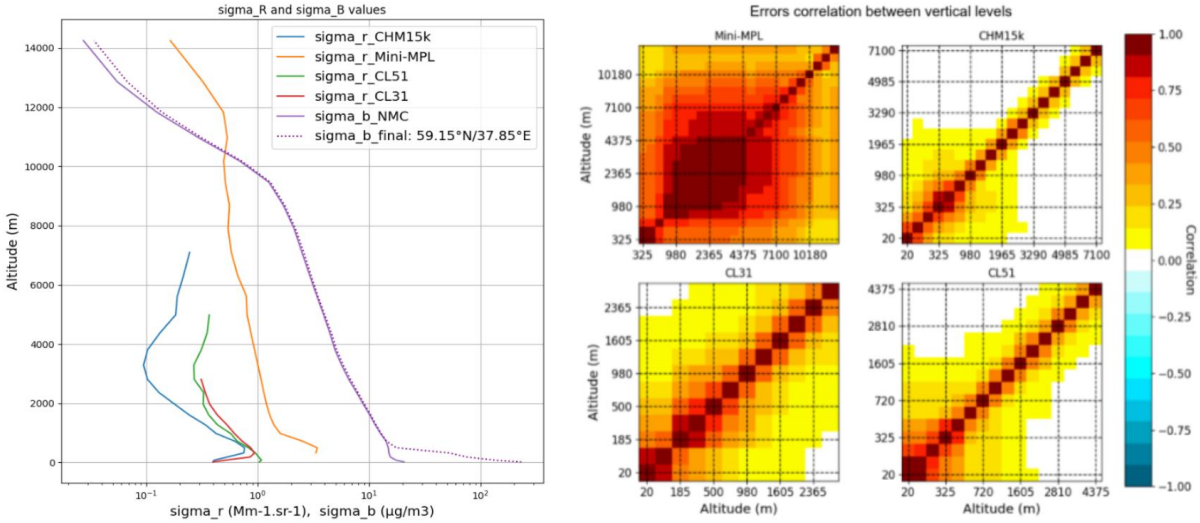

Figure 3: Profiles of observation and background error standard deviations (left) and observation error vertical correlations (right).

3.3.3 Background errors

Similarly to observations errors, the errors related to the background state (aka first-guess of the assimilation) need to be properly described. We started with a very simple way to represent the background error standard deviations: a percentage of the model concentration is used. Again, in this part of the study, the control variable is the total concentration of all aerosols (all types of aerosols and all sizes; name is TOTAM). A more advanced method is the so-called NMC method (Parrish and Derber 1992), which uses differences between +36h and +12h forecasts valid for the same date to sample the forecast error. After several attempts (not shown here), we decided to use for the background error standard deviations, the (constant) vertical profile diagnosed from the NMC method to which 25% of the local concentration of TOTAM is added. The NMC value and an example of the final background error standard deviations (at a given location and date) are given in Figure 3.

3.3.4 Analysis and forecast scores

An assimilation experiment with the best settings for the observation and background errors has been run over a 5 months period from January 1st to May 31st 2024. A control experiment with no assimilation is also run.

First, an evaluation of the quality of the analyses against EEA observations at surface and AOD observations from AERONET is performed. AERONET is a network of ground-based sun photometers which measure atmospheric aerosol properties. The time series of concentration of PM10 at the analysis time is given in Figure 4. Overall, the assimilation of e-profile data leads to an increase in concentrations of particulate matters at the surface, both

in PM10 and PM2.5. This helps reducing the negative bias that MOCAGE has on PM10, but it increases the positive bias already existing for PM2.5. Major events seem to be well reproduced thanks to the assimilation of e-profile data, mainly for the dust export episode occurring at the beginning of the evaluation period, in January.

Synthetic scores are given in Table 1. They confirm the behaviour already described. The correlation is improved for both species. Similarly, the total AOD bias is slightly increased while the correlation is slightly improved.

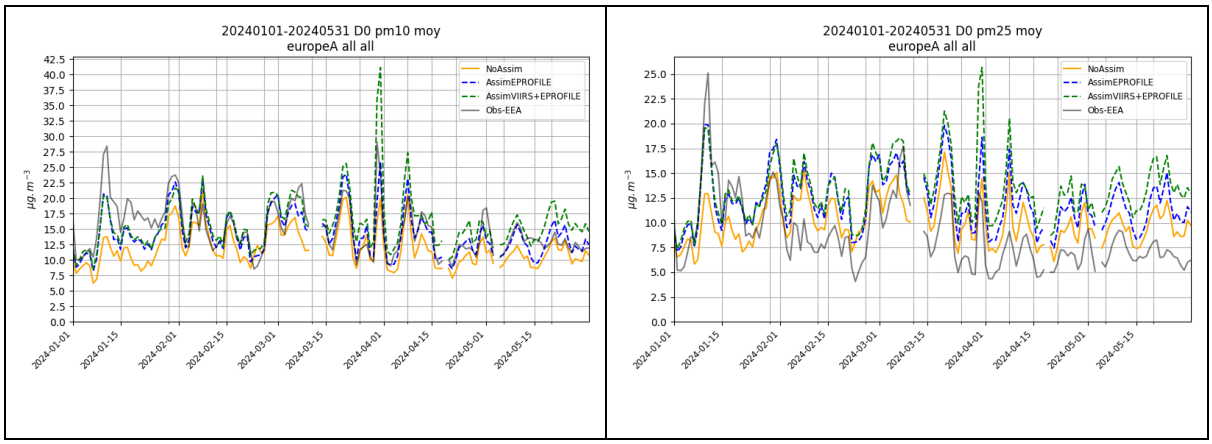

Figure 4: Time series from 01.01.2024 to 31.05.2024 for PM10 (left panel) and PM2.5 (right panel) concentrations at the surface. Observations from EEA are in grey, values from the control experiment (noAssim) in orange, e-profile assimilation in blue and joint assimilation of e-profile and VIIRS in green.

	PM10 at surface from EEA *µg.m^{-3}*		PM2.5 at surface from EEA *µg.m^{-3}*		AOD from AERONET *unitless*	
	NoAssim	Assim EPROFILE	NoAssim	Assim EPROFILE	NoAssim	Assim EPROFILE
Bias	-3.0	-0.67	1.1	3.7	0.022	0.03
RMSE	15	14	8.6	9.2	0.086	0.089
Correlation	0.5	0.57	0.52	0.58	0.71	0.73

Table 1: Synthesis of analysis scores against independent observations.

An illustration of how the assimilation of e-profile observations can improve the overall aerosol total concentration and its vertical distribution is given in Figure 5, which shows the temporal evolution of the vertical attenuated backscatter at the Klippeneck station (in Baden-Württemberg, Germany) over 15-17 March 2022, which corresponds to a former desert dust episode over Europe. Even though the assimilation of e-profile data still misses some part of the event, the vertical distribution and the amplitude of the concentration are well reproduced in the second part of the event.

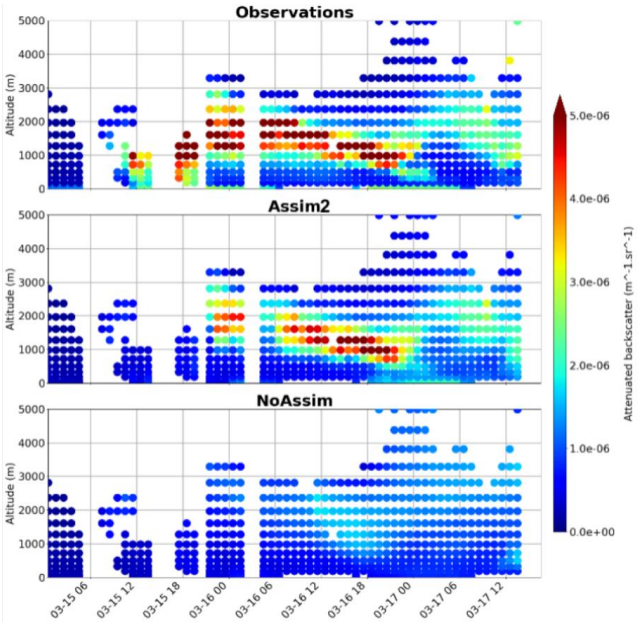

Figure 5: Attenuated backscatter at Klippeneck from 15 th to 17 th March 2022.

Now, the impact on the quality of the 96h forecasts that are initialised from the analyses assimilating e-profile has been assessed. Similar features to those for the analyses have been found. We investigated on how long the effect of the assimilation would last in the forecast. In Figure 6 the evolution of the bias against EEA observation is given with respect to the forecast range. Most of the impact is noticed in the early forecast ranges, with a slow decay. During the second day of forecast, the impact can still be observed but at with a very low amplitude. Almost no differences are found after +48h forecast range. The findings are similar for the correlation metric.

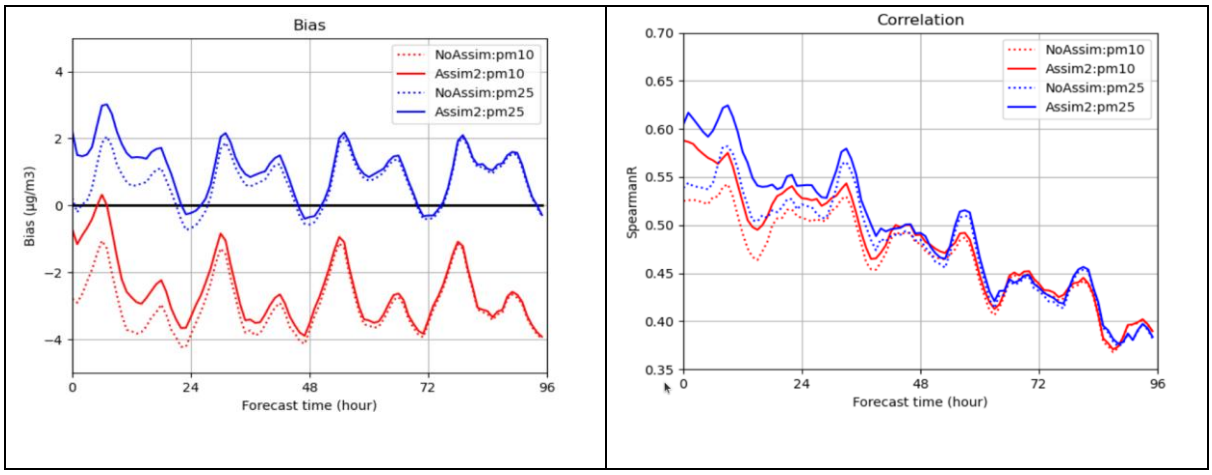

Figure 6: Evolution of scores against EEA observation with respect to the forecast range (bias on left and correlation on right).

3.3.5 Conclusion on e-profile assimilation

The data from the e-profile network need a careful preprocessing step to get rid of spurious and unwanted parts of the measurements and focus on the aerosol signal. They provide a useful information with vertical distribution, up to different vertical ranges depending on the actual sensor type. Once this first and crucial step is achieved, a proper description of the observation errors is needed in the assimilation algorithm (here an hourly 3D-Var) so that the minimisation process can extract the information on the vertical.

In the frame of the Horizon Europe project which aims at improving the CAMS services, in particular the regional service in the task, the quality of particulate matter at surface has been evaluated, both at analysis time and over the full forecast range. Mainly, the assimilation of e-profile data increases the concentration of aerosols in the atmosphere and also at surface level. It helps improving the negative bias existing in MOCAGE for PM10, but adds to the positive bias in PM2.5. The correlation to independent verification data (EEA surface observations and AODs from AERONET) is improved. These features last up to 36-48h of forecast range, with a smooth decay. No impact is found after +48h forecast range.

4 Assimilation of VIIRS AODs

4.1 MONARCH

The assimilation of VIIRS total AOD was implemented in the MONARCH-DA data assimilation system, used at BSC for the CAMS regional reanalysis.

Data assimilation of VIIRS AOD had already been implemented in MONARCH-DA and is used for products such as the Barcelona Dust Regional Forecast (BDRC), but this was limited to dust particles. This was done through a pre-filtering of the VIIRS observations, selecting only those with (likely) high dust load, and then performing the assimilation only on the dust tracers (8 size bins) of MONARCH, ignoring the potential contribution of other aerosol species to the observations.

We therefore had three specific goals in this task:

- Implement and validate the assimilation of total AOD observations, accounting for the eight aerosol species (distributed in 34 bins) accounted for in MONARCH;
- Implement the capacity to simultaneously assimilate surface and satellite observations;
- Assess the use of these AOD observations for improving the forecasting performance of the system.

Two sets of experiments were performed, covering two one-month periods: January 2024 and September 2024. The former was chosen because it covered of a major Saharan dust event, the second one covers important forest fires in Portugal, as well as two events of long-range transport of aerosols in Northern Europe. In this report we focus on the experiments covering September 2024, as the VIIRS coverage in January was rather low.

4.1.1 Observations

We assimilated retrievals from the Level 2 NOAA-20 VIIRS Deep Blue Aerosol 550 nm AOD product.

The preprocessing was based on the one used for the assimilation of dust AOD at BSC: The retrievals were pre-averaged on the MONARCH grid, so that there is a maximum of one observation per grid-cell. The model error is set to 0.01 m and the observational error set mainly proportionally to 20% of the observed value (higher for very low AOD).

We also assimilated surface PM10 observations from EIONET surface air quality monitoring networks. The dataset corresponds to the one prepared for the CAMS VRA reanalysis.

4.1.2 MONARCH-DA data assimilation framework

The reanalysis has been produced using the Multiscale Online Nonhydrostatic AtmospheRe CHemistry model (MONARCH; Pérez et al., 2011; Haustein et al., 2012; Jorba et al., 2012; Spada et al., 2013; Badia et al., 2017; Klose et al., 2021), which consists of advanced chemistry and aerosol packages coupled online with the Nonhydrostatic Multiscale Model on the B grid (NMMB; Janjic and Gall, 2012).

In this work, we made use of the setup developed for the CAMS regional air quality reanalysis, which runs at a 0.2° horizontal resolution, on a rotated latitude-longitude grid, and 24 vertical levels, and IFS boundary conditions (with chemical boundary conditions from CAMS global).

The data assimilation framework is based on that described in Di Tomaso et al., 2022: the aerosol concentration fields are optimized using a Local Ensemble Transform Kalman Filter

(LETKF), from a 12-member forecast ensemble, with perturbations applied to calibration factors of the dust emission model and to anthropogenic emissions. The DA controls the total aerosol concentration, in four dimensions (time, lat, lon and model level). The analysis concentrations for each tracer are then obtained by scaling the forecast tracer concentration by the ratio of analysis over forecast total concentration.

The LETKF essentially performs a local data assimilation experiment for each model grid cell, accounting for the influence of observations around each grid cell. The observation influence is controlled by a Gaussian localization function, controlled by localization coefficients which scale up the observation uncertainty depending on their distance (in space and time) to the center of the grid cell. We implemented the possibility to set the localization coefficients per observation type:

– The vertical localization was set to 3 levels for surface observations (limiting their influence to the lower levels), but wasn't used for VIIRS retrievals (since they are sensitive to the whole atmospheric column);
– The horizontal localization was set to 3 grid cells (approx. 0.6°) for surface data, and to 5 grid cells (approx 1°) for VIIRS;
– The temporal localization was set to 3 hours in both cases.

The settings were chosen rather conservatively, based on the existing setup. It is however clear from the next section that at least the temporal localization will need to be increased.

4.1.3 Results

4.1.3.1 Joint assimilation of VIIRS AOD and surface PM10 observations

Three "base" experiments were performed for September 2024: **SP** (reference setup, assimilating only surface PM10 data); **SV** (assimilation of VIIRS data only) and **SPV** (joint assimilation of surface and VIIRS data). The experiments were performed in an "offline" mode, where the assimilation at day *n* is not propagated to day *n+1*. This allows performing multiple assimilation experiments sharing the same forecast ensemble. Forecasts with online assimilation cycle are shown in Section 4.1.3.2

We assessed the capacity of each of the DA experiment to fit both the surface (EIONET) and satellite (VIIRS) observations. VIIRS observations are assimilated in SV and SPV and PM10 data are assimilated in SP and SPV, so this is not an independent validation, rather a consistency check.

Daily fit statistics (mean bias, root mean square error (RMSE) and correlation coefficient) are shown in Figure 7. Overall, the impact of VIIRS data on the fit to surface observations is rather limited: the huge bias reduction around September 20 doesn't correspond to a RMSE reduction in SV, therefore the errors simply compensate each other better in the analysis than in the forecast. On the other hand, assimilating surface observations only (as is currently done in the CAMS regional air quality reanalysis) leads to a slight improvement in the fit to VIIRS data. The SPV experiment achieves comparable fit to VIIRS than SV, and to PM10 data than SP, therefore there is at least not a significant penalty in performing a joint assimilation.

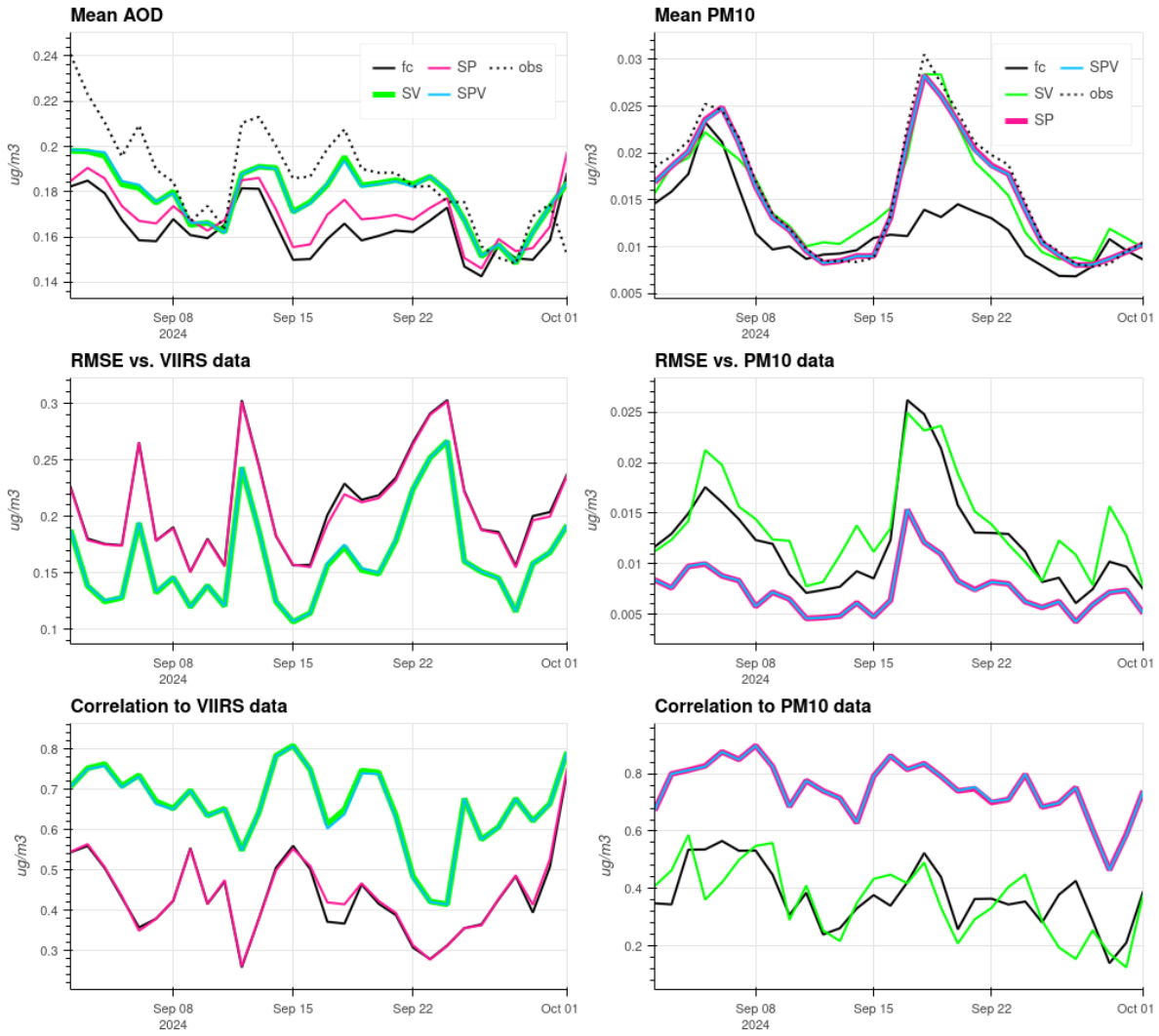

Figure 7: Fit statistics against surface (PM10, in mg/m3) and VIIRS AOD observations obtained in the "offline" experiments (SP, SV and SPV). Some lines were made thicker to make them visible when they overlap with others.

Two major events are visible in the surface observations in September 2024:

- A first peak of PM10 concentration was recorded around September 6, spanning roughly over Germany and Poland. This event was somewhat well captured by the MONARCH forecast ensemble, which points to long-range transport from the Eastern boundary of the domain. The event appears earlier in the VIIRS retrievals, over Ukraine and Belarus, where there is no PM10 data.
- A second event, around September 19, also spans most of Northern Europe plus the Western part of the Iberian Peninsula. It follows, in time, major forest fires in Portugal (https://www.copernicus.eu/en/media/image-day-gallery/severe-wildfires-portugal-september-2024). However the forecast largely underrepresented the fires, and it is somewhat unclear if there was also some contribution from outside the domain.

Since our focus is rather on the DA than on the model itself, we focused on the first event.

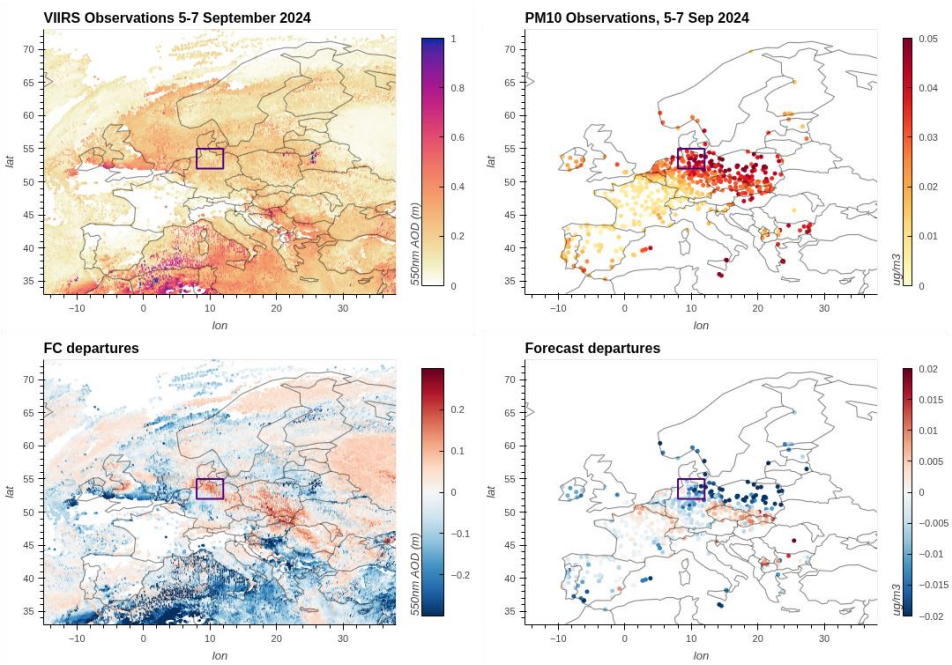

Figure 8: Observed and modelled AOD (left) and PM10 (right) over Northern and Central Europe on 5-7 September 2024. The model values are shown as departures from the observations. The rectangular area on each plot is the one used for computing the profiles in Figure 10.

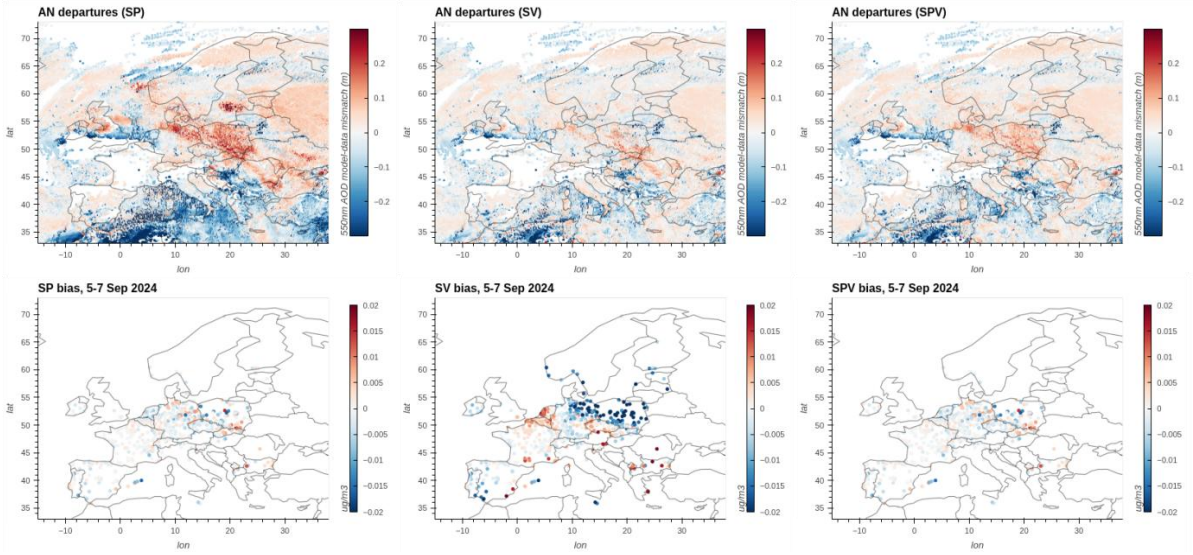

Figure 9: Analysis departures corresponding of the SP, SV and SPV experiments, corresponding to the forecast departures shown in Figure 8.

Figure 8 shows the observations corresponding to that event, and the model-data mismatches on the bottom. Interestingly, the event is barely visible in the AOD retrievals, but very prominent in the PM10 observations. On the contrary, the forecast underestimated the event on the ground and underestimated its consequences on AOD. The DA experiments are able to fit the data, although SPV still somewhat struggles to fit the VIIRS AOD (Figure 9).

We analyzed the vertical profiles from the assimilation experiments in a few interesting locations. Figure 10 shows vertical profiles of AOD in the rectangular area highlighted in Figure 8. There, the forecast simultaneously underestimated the surface observations, and overestimated the VIIRS retrievals.

The SPV experiment manages to accommodate these contrary constraints by adjusting the vertical profile of aerosols, following roughly the profile obtained in the SP (PM10-only) assimilation for the lowest levels, and then the profile from the SV (VIIRS-only) one above the tenth level. The increased aerosol concentrations in the lowest model levels in SVP, compared to SV, is not compensated by a more significant reduction in higher altitude, resulting in a higher total column AOD in SPV than in SV (though this is likely not a frequent issue, based on the domain-wide statistics shown in Figure 7).

Practically, this means that the DA is essentially capable of using PM10 observations to constrain the surface and VIIRS observations to constrain the free troposphere, the main benefit from the latter is likely improved forecasting performance, if that updated tropospheric information can be carried forward to the next day.

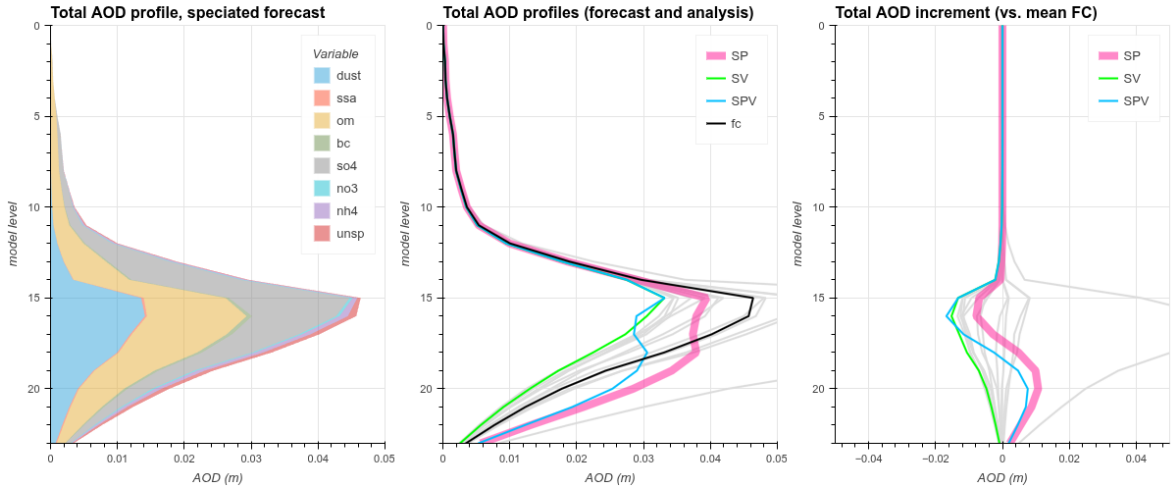

Figure 10: Vertical profiles of AOD over Northern Germany, on September 6, 2024, at 12:00. The left diagram shows the contribution of each aerosol species to the forecast AOD. The center column compares the analyses (SP, SV and SVP) to the mean forecast (fc), and the plot on the right shows the difference to the mean forecast. Grey lines correspond to the twelve forecast members.

4.1.3.2 Impact on forecast performance

We implemented a set of "online" experiments, where the forecast of day *n+1* is initialized based on the atmospheric aerosol concentrations inferred at the analysis of day *n*. This could theoretically enable making better use of the information on the free tropospheric aerosol content provided by VIIRS.

Two experiments were conducted: SV_ol and SPV_ol, corresponding respectively to SV and SPV, but with forward propagation of the analysis. Fit statistics to VIIRS AOD and EIONET PM10 data are shown in Figure 11.

The forecasts of the SPV_ol experiment achieves better correlation to PM10 observations than the "offline" forecast (used in SV, SP and SPV) does. However, the impact of VIIRS observations is rather negligible: this is due to the fact that the observations are generally around 12:00 UTC, so their influence on the analyzed concentrations at midnight (which is used to initialize the next forecast step) is negligible.

The issue is clearly the temporal localization of the VIIRS observations, which is too strong, and will be adjusted in a re-run of these experiments.

While this propagation of the analysis does appear to have an importance for the quality of the forecast, the impact on the assimilation at day *n+1* is largely negligible, so the "offline"

approach, used in the previous section and which is much simpler to implement, remains valid when the forecast is not the main aim (e.g. when conducting reanalysis).

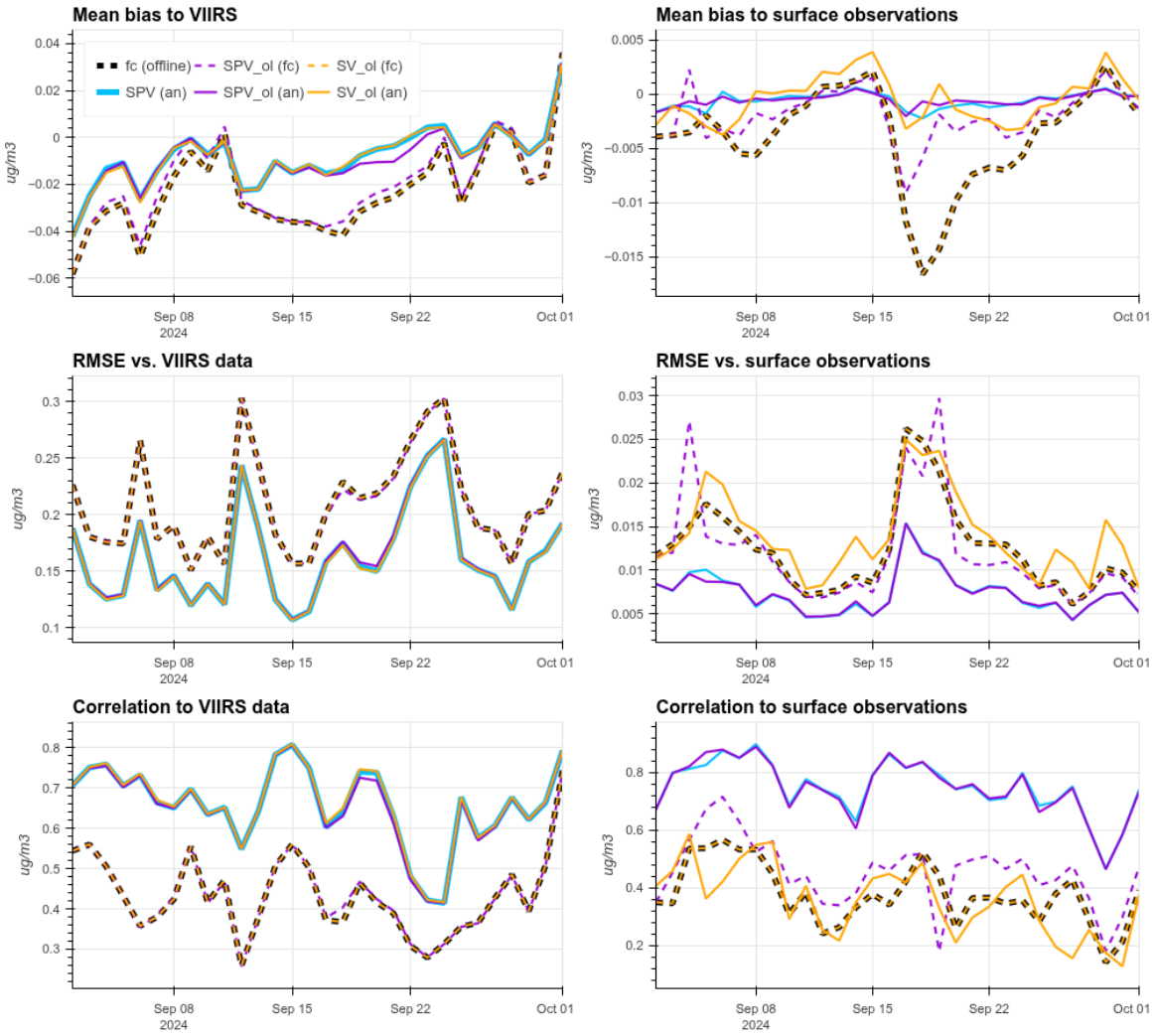

Figure 11: Fit statistics to VIIRS (left) and surface PM10 (right) observations, for the forecast and analysis of the SV_ol, SPV_ol and SPV experiments

4.1.4 Conclusions

We have implemented a data assimilation chain capable of assimilating total AOD retrievals from VIIRS in MONARCH-DA. The system has shown promising results although an integration in the current CAMS operational products appears premature.

One of the main issues has been the computational cost of the experiments. This is largely due to inefficiencies in the I/O of MONARCH-DA, which weren't major limitations when performing DA experiments on one (PM10) or eight (dust) MONARCH tracers, but become a major bottleneck when accounting for all 34 tracers, and with a larger 12-member ensemble, with more than 40 minutes taken just to read the ensemble for each day of assimilation. There however is good scope for improvement on that aspect.

VIIRS observations appear to provide limited information on surface PM10 concentrations, especially when there are already robust constraints from surface monitoring networks. However, they do constrain the troposphere, which our DA framework should be able to use to improve the forecast, after further tuning of the data assimilation parameters.

4.2 SILAM

4.2.1 Methods

VIIRS AOD is assimilated using the Ensemble Kalman Filter (EnKF). The ensemble is formed by perturbing the emissions of all species, the boundary condition for all species, and the time of the meteorological data. The emissions were perturbed by applying a spatially correlated emission scaling factor, with a horizontal correlation distance of 300 km and correlation between neighbouring cells of 0.6. The amplitude of the perturbation was set to 0.5. The emissions were perturbed only in the horizontal plane, i.e. column-wise. The boundary condition was perturbed in a similar way, but with the correlation distance being set to 600 km, the nearest-neighbour correlation to 0.95, and the amplitude to 0.1 (0.02 for ozone). Moreover, an interspecies correlation was forced by selecting the boundary condition perturbation for each species to equal the average of a perturbation common to all species and a species-specific perturbation (as this is computationally much more efficient than computing a covariance matrix that in addition to the spatial dimensions would also depend on the species dimension). The standard deviation of the perturbation of the time of the meteorological data was set to 60 minutes. The ensemble size was selected to be 32. The state vector was set to be composed of the in-air concentrations of all aerosol species in SILAM, and the following gases: SO2, NH3, toluene and xylene.

Three separate cases were assimilated: AOD from the Dark Target (DT) algorithm only, AOD from the Deep Blue (DB) algorithm only, and DT and DB AOD simultaneously. Thinning of the retrievals was performed by clustering them into 0.25 degree x 0.25 degree cells (same resolution as in the model), and the median retrieval in each cluster was selected as the thinned value. The retrieval error for the thinned DB and DT data was set to equal 0.2 times the value plus a constant error of 0.07. In addition to the assimilation cases, a control run was performed using the same model setup but without assimilation.

The model domain of the assimilation covered the standard domain of the CAMS regional forecast, but was set to extend higher up vertically, i.e. to about 170 hPa, and to consist of 18 vertical layers compared to 10 vertical layers in the standard SILAM regional forecast. The model was run at a 0.25 degree x 0.25 degree resolution using ERA5 meteorological data. Compared to the IFS forecasts from recent years, ERA5 performs relatively similarly when used to drive SILAM, although often yielding marginally worse skill scores. The emissions used were the CAMS regional emissions v. 8.1, together with the other standard emissions of the SILAM CAMS regional forecast, except that the fire emissions were based on the most recent iteration of IS4FIRES instead of GFAS.

September 2024 was selected for evaluation of the assimilation setups. A seven day spinup period, also including assimilation, was performed for the end of August.

4.2.2 Results

The performance of the assimilation was evaluated against the control run for in-situ data consisting of EEA observations of the standard air-pollutants, and against AERONET level 1.5 AOD. The AERONET AOD was mapped into 550 nm equivalent AOD using the calculation of an Angstrom exponent (AE), following the same approach as used in the SDS-WAS evaluation

(except that no screening based on the AE was performed). In addition to the analyses with assimilation of DB, DT and DB & DT AOD, also forecasts initialized at 00:00 UTC from the DB & DT analysis are evaluated, separately for the first day of forecast and the second day of forecast.

The results of the comparison against AERONET AOD are summarized in Table 2. All assimilation setups significantly improve the RMSE and correlation against AERONET AOD, although they are not improving the negative bias (and are in fact slightly increasing it). The base case AOD and the assimilation increments are presented in Figure 12, while Figures 13 and 14 show the same for surface PM2.5 and PM10.

Tables 3 and 4 present evaluation against in situ EEA PM2.5 and PM10, respectively, for stations used for the operational evaluation of the CAMS regional forecast. As opposed to the AERONET scores, Tables 3 and 4 present the station averaged RMSE and correlation, as these scores are more robust than the full RMSE and correlation due to some stations exhibiting data quality issues.

Table 2: Comparison of the base case and the assimilated cases against AERONET AOD, together with the first and second days of forecasts initialized from the DB & DT analysis.

	mean obs	mean mod	RMSE	corr
base	0.137	0.122	0.081	0.675
DB	0.137	0.117	0.069	0.770
DT	0.137	0.118	0.068	0.776
DB & DT	0.137	0.118	0.066	0.791
first day from DB & DT	0.137	0.118	0.071	0.747
second day from DB & DT	0.137	0.121	0.076	0.713

Table 3: Comparison of the base case and the assimilated cases against EEA PM2.5 for operational evaluation stations, together with the first and second days of forecasts initialized from the DB & DT analysis. The values presented are means for individual stations. Where relevant, the unit is µg/m3.

	mean obs	mean mod	RMSE	corr
base	8.30	10.26	6.83	0.716
DB	8.30	9.31	5.48	0.745
DT	8.30	9.43	5.70	0.741
DB & DT	8.30	9.35	5.62	0.742
first day from DB & DT	8.30	9.54	5.91	0.735
second day from DB & DT	8.30	9.94	6.45	0.727

Table 4: Comparison of the base case and the assimilated cases against EEA PM10 for operational evaluation stations, together with the first and second days of forecasts initialized from the DB & DT analysis. The values presented are means for individual stations. Where relevant, the unit is µg/m3.

	mean obs	mean mod	RMSE	corr
base	20.64	15.48	16.29	0.671
DB	20.64	14.41	15.06	0.691
DT	20.64	14.55	15.23	0.687
DB & DT	20.64	14.46	15.23	0.685
first day from DB & DT	20.64	14.85	15.59	0.686
second day from DB & DT	20.64	15.19	16.00	0.679

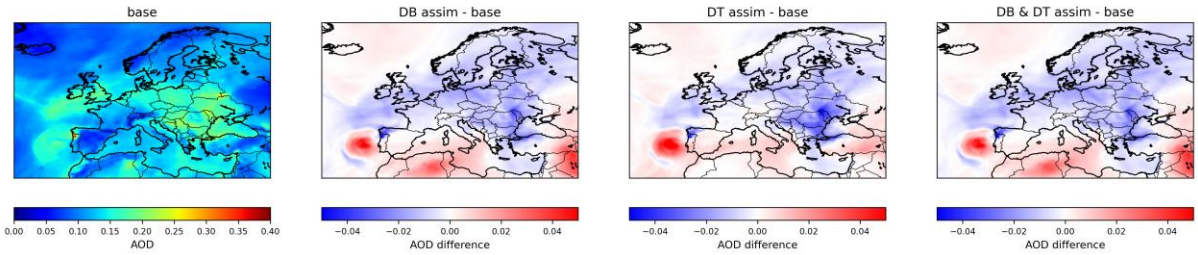

Figure 12: Base case AOD without assimilation from the SILAM model for September 2024 (left), and the increments for DB, DT, and DB & DT assimilation.

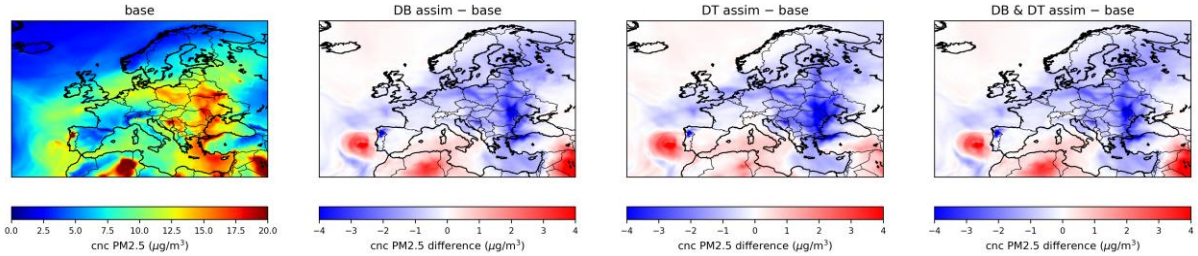

Figure 13: Base case surface PM2.5 concentration without assimilation from the SILAM model for September 2024 (left), and the increments for DB, DT, and DB & DT assimilation.

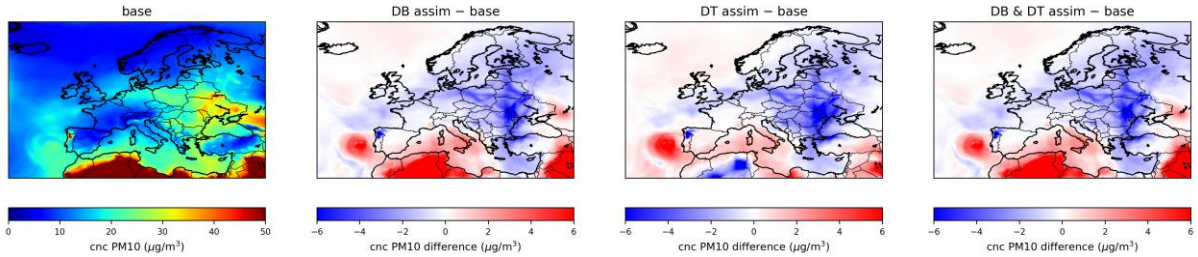

Figure 14: Base case surface PM10 concentration without assimilation from the SILAM model for September 2024 (left), and the increments for DB, DT, and DB & DT assimilation.

4.2.3 Conclusions

Assimilation of VIIRS AOD improved SILAM performance against AERONET AOD and against surface PM2.5 and PM10. As is evident for Tables 2-4, the improvement was partly propagated into the forecast initialised from the analysis for the two first days of forecast, initialised at midnight. The third day of forecast was not evaluated, but extrapolating the decay of the performance improvement from days 1 and 2 indicates that there would not be any meaningful improvement after two days of forecast. Adjusting the assimilation parameters could potentially yield even more improvement. Although generally considered inferior to the DT algorithm, the DB algorithm showed its strength in the assimilation experiment due to its ability to obtain AOD retrievals over desert surface.

A similar setup has been previously tested for SILAM with MODIS instead of VIIRS AOD, yielding similar results for a full year of assimilation. That simulation indicated that assimilating AOD has the potential to slightly improve surface ozone as well, as the photolysis reactions depend on the AOD in SILAM, but in the VIIRS test runs for September only, no meaningful improvement for surface ozone scores was achieved.

4.3 MOCAGE

4.3.1 Observation preprocessing

VIIRS AODs are already assimilated in MOCAGE global domain. The data flow used is the NOAA NRT dissemination with AODs provided at the pixel resolution, for each operational NOAA satellite embarking VIIRS. In MOCAGE global domain, our preprocessing consists in super-obbing to the model resolution by averaging all the available VIIRS pixels within each MOCAGE grid cell. During the present study, we first started with the same approach: super-obbing VIIRS AODs by averaging the data in each MOCAGE 0.1 x 0.1 model grid cell. After several attempts (not shown here), we moved towards another way of super-obbing, by using the 90th percentile value of the VIIRS AODs present in each MOCAGE grid cell. Obviously, this choice led to higher values used in the assimilation. No further preprocessing is applied.

4.3.2 Observation and background errors

The same background error setting is used as in section 3.3.3 for the e-profile assimilation.

For the observation errors, a Desroziers diagnostic has also been applied. As VIIRS observations have been used both over land and sea, from both S-NPP and NOAA-20 satellites, we have computed different values of observation error standard deviation for each satellite and each surface type.

For S-NPP, the standard deviation used is 0.0434 over land and 0.0277 over sea.

For NOAA-20, the standard deviation used is 0.0536 over land and 0.0249 over sea.

Contrary to what is done in IFS-Compo (CAMS global), no bias correction is applied to VIIRS data in these trials, as it would require much more work to implement a variational bias correction in MOCAGE; the domain being regional and not global is also a limitation for a bias correction evaluation and usage.

4.3.3 Impact of assimilating VIIRS only

In this section, we evaluated the impact of assimilating VIIRS only over the month of January 2024. As can be seen in Figure 15 which depicts the time series for concentrations of particulate matter at surface both in analyses and EEA observations, the impact of assimilating VIIRS AODs is very modest, mostly neutral. Figure 16 shows how the scores vary according to the analysis time. For bias, the behaviour is rather consistent over the day. For correlation, one can notice that the minimum value in the VIIRS assimilation experiment is obtained for the 12-14 UTC time window, which corresponds to the VIIRS overpass time. This can indicate that the information provided by VIIRS, integrated over the troposphere, is not consistent with the information at surface.

Verification of analyses against AERONET AODs also shows a neutral impact (not shown).

We also verified the quality of the subsequent forecasts. Forecast scores over the first 24 hours of forecast range are given in Table 5. As for the analysis, the assimilation of VIIRS AODs has a neutral impact on forecasts.

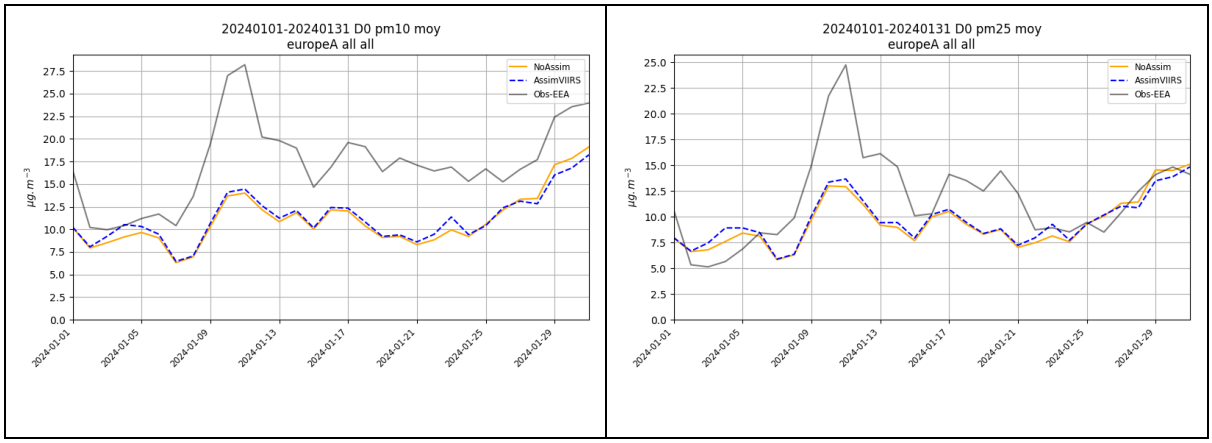

Figure 15: Time series from 01.01.2024 to 31.01.2024 for PM10 (rp. PM2.5) concentrations at surface (left, rp right panel). Observations from EEA are in grey, values from the control experiment (noAssim) in orange, VIIRS AOD assimilation in blue.

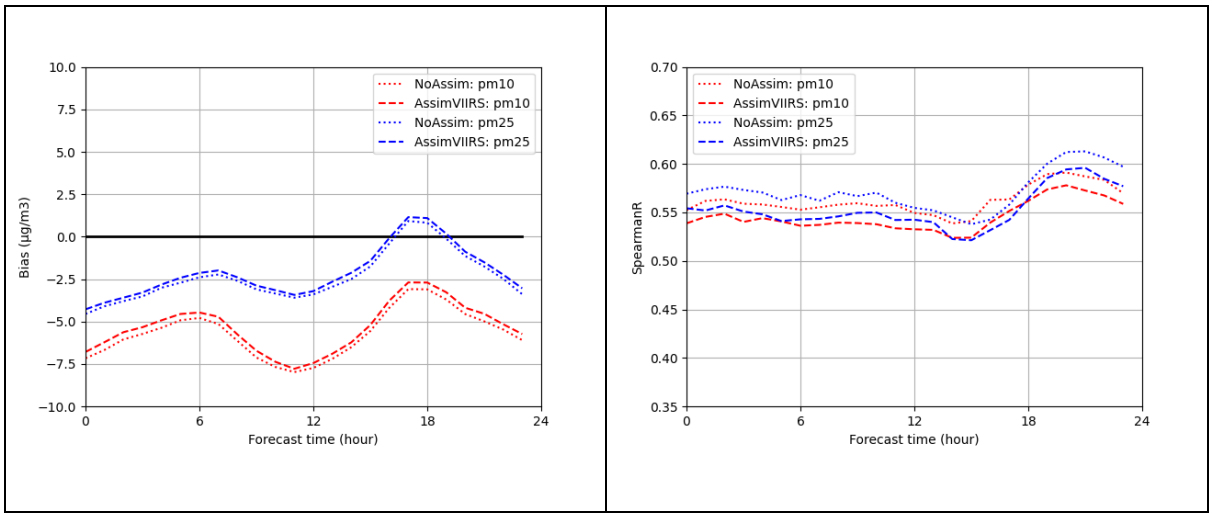

Figure 16: Evolution of scores against EEA observation with respect to the analysis time (bias on left and correlation on right), average scores over the period 01.01.2024 to 31.01.2024.

	PM10 at surface from EEA *μg.m^{-3}*		PM2.5 at surface from EEA *μg.m^{-3}*		AOD from AERONET *unitless*	
	NoAssim	Assim VIIRS	NoAssim	Assim VIIRS	NoAssim	Assim VIIRS
Bias	-5.6	-5.4	-2.3	-2.1	0.025	0.027
RMSE	15	15	11	11	0.05	0.049
Correlation	0.55	0.53	0.55	0.54	0.58	0.58

Table 5: Synthesis of forecast scores against independent observations.

4.3.4 Impact of joint assimilation of VIIRS and e-profile

In order to evaluate the potential synergy of ground based and space borne remote sensing of aerosols for the forecast of aerosol concentration at surface, we set up an experiment that assimilates both e-profile data and VIIRS observations. We use the preprocessing of e-profile described in section 3.2 and the VIIRS preprocessing described in section 4.3.1. The background errors are the same as previously used in MOCAGE for this study. The observation error description for VIIRS and e-profile are those explained in sections 4.3.2 and 3.3.2.

We used here the 5-month period from January to May 2024 to evaluate this setting.

The recap of the evaluation of analyses against independent observations (surface concentrations of PM from EEA and AODs from AERONET) is given in table 6. The joint assimilation increases even more the concentrations of PM, both at surface and integrated on the vertical as AOD. Biases are thus higher for all verification data. The correlation is degraded when compared to the assimilation of e-profile only, but is still better than the correlation obtained without any assimilation. Figure 17 shows the values of the scores depending on the analysis time. As for the assimilation of VIIRS only, a degradation of the scores occurs in coincidence with the VIIRS instruments overpass of the domain, indicating a discrepancy in the information extracted from these observations compared to others like e-profile and EEA surface observations.

	PM10 at surface from EEA *µg.m^{-3}*			PM2.5 at surface from EEA *µg.m^{-3}*			AOD from AERONET *unitless*		
	NoAssim	Assim EPROFILE	Assim EPROFILE+VIIRS	NoAssim	Assim EPROFILE	Assim EPROFILE+VIIRS	NoAssim	Assim EPROFILE	Assim EPROFILE+VIIRS
Bias	-3.0	-0.67	1.7	1.1	3.7	4.3	0.022	0.03	0.062
RMSE	15	14	16	8.6	9.2	10	0.086	0.089	0.1
Correlation	0.5	0.57	0.51	0.52	0.58	0.54	0.71	0.73	0.72

Table 6: Synthesis of analysis scores against independent observations (table 1 with additional columns for joint assimilation), from 01.01.2024 to 31.05.2024.

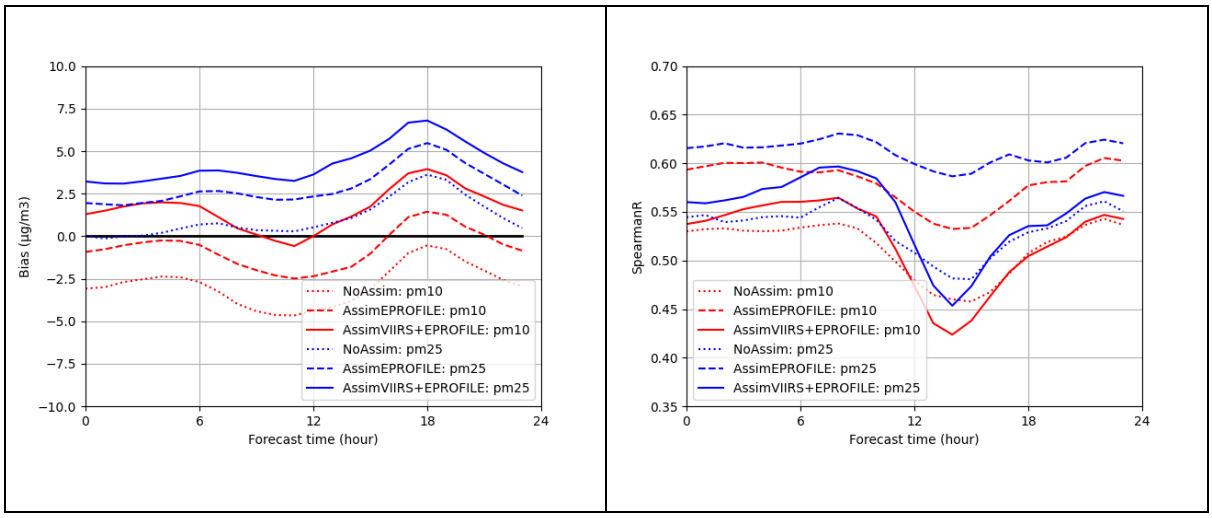

Figure 17: Evolution of scores against EEA observation with respect to the analysis time (bias on left and correlation on right), average scores over the period 01.01.2024 to 31.05.2024.

When the forecasts are evaluated, we can observe a similar behaviour. In Figure 18, the time series of concentrations of PM at surface are given for the month of January 2024. The quality of the forecasts initialised from VIIRS+e-profile assimilation and from e-profile only assimilation are very close to each other, both being better thatn the no assimilation run.

The forecast scores in Table 7 highlight again that biases and RMSE against EEA surface concentrations are similar for both assimilation runs. Correlations are a bit decreased in the case of the joint assimilation compared to the assimilation of e-profile only.

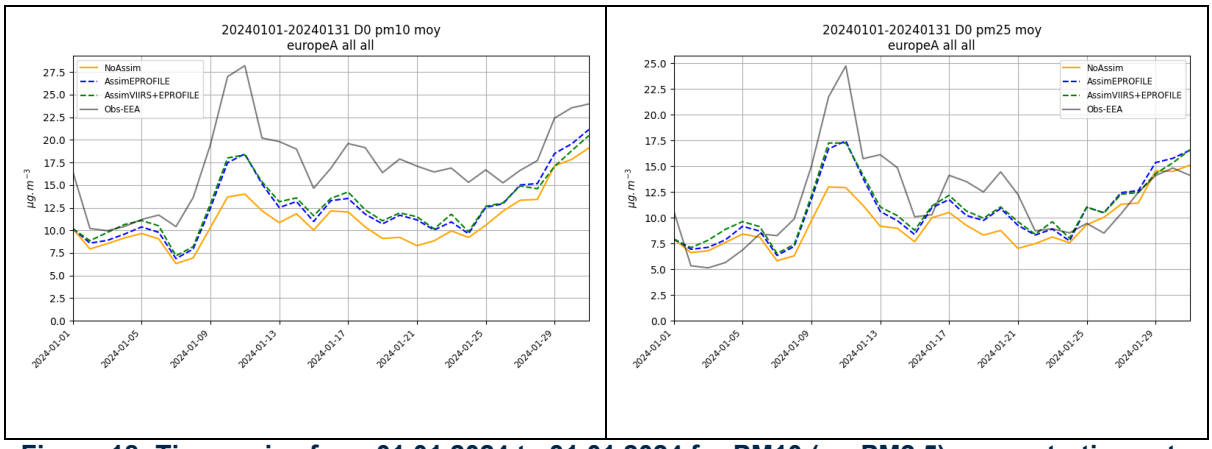

Figure 18: Time series from 01.01.2024 to 31.01.2024 for PM10 (rp. PM2.5) concentrations at surface (left, rp right panel). Observations from EEA are in grey, forecasts from the control experiment (noAssim) in orange, e-profile assimilation in blue and joint assimilation of e-profile and VIIRS in green.

	PM10 at surface from EEA *µg.m^{-3}*			PM2.5 at surface from EEA *µg.m^{-3}*			AOD from AERONET *unitless*		
	NoAssim	Assim EPROFILE	Assim EPROFILE+VIIRS	NoAssim	Assim EPROFILE	Assim EPROFILE+VIIRS	NoAssim	Assim EPROFILE	Assim EPROFILE+VIIRS
Bias	-5.6	-4.3	-4.1	-2.3	-0.97	-0.82	0.025	0.029	0.033
RMSE	15	14	14	11	10	10	0.046	0.048	0.052
Correlation	0.55	0.58	0.57	0.55	0.60	0.59	0.62	0.63	0.58

Table 7: Synthesis of first 24h forecast scores against independent observations, from 01.01.2024 to 31.01.2024.

4.3.5 Conclusions on VIIRS assimilation trials

In MOCAGE, the assimilation of VIIRS AODs has proven to bring very few impact on surface concentration analyses and forecasts. The joint assimilation of VIIRS AODs together with e-profile data has shown very little impact compared to the assimilation of e-profile only. No impact is found in the evaluation against AERONET data. This finding is in opposition to what has been found in the assimilation of VIIRS AODs in the global domain of the MOCAGE model, where a large improvement is found. The reason may be that a large part of aerosols present in the regional domain of MOCAGE are coming from the lateral boundary conditions, which are provided by IFS-Compo (CAMS global), that already has a very good quality.

5 Conclusion

In this task, we have explored the potential benefits of assimilating ground-based lidars and ceilometers from the e-profile network and satellite total AODs from VIIRS sensors to improve the aerosol representation and forecasts of particulate matter at surface.

The assimilation of e-profile data needs a careful preprocessing of the data. No station has to be discarded a priori, but some consistency check has to be done between the altitude of the ground represented in the model in which the data are assimilated and the actual altitude of the station. Then, the data have to undergo further screening for clouds and rain, as well as noisy data.

Thanks to e-profile data, both the vertical structure of aerosols and their concentrations can be modified during the assimilation. In our case, it led to an increase of the concentrations in average, thus to an increase of the total AOD and PM concentrations at surface. These corrections to the atmospheric concentrations also led to improvements in the analysis and forecast scores. The improvements last at least 24h and span, to a weaker extent, up to 48h of forecast range.

A first version of the assimilation of e-profile data in MOCAGE has been transferred to operations during the CAMEO project. Nevertheless, the readiness of the other models within the regional ensemble may be much lower.

The assimilation of VIIRS AODs in 3 different models and assimilation settings provided positive to neutral impact, even if the impact of VIIRS assimilation on surface concentration is not direct. VIIRS AODs have several advantages, like a wide coverage of the domain, or various available algorithms (Deep Blue and Dark Target). Further work is needed to refine the assimilation parameters, like bias correction, for instance.

Joint assimilations of VIIRS AODs have been evaluated, together with surface observations in MONARCH and with e-profile data in MOCAGE. In both cases, the results are still exploratory and more work is needed.

In general, the level of maturity of the assimilation of VIIRS AODs in regional models seems not sufficient to be transferred into operations for the time being. Moreover, the 3 participating models in this task may not be representative of the level of readiness of the full team of regional models.

For both instruments, this study paved the way for fruitful innovations in the frame of the regional service of CAMS. It is important to note that much more work is needed to have all models reaching the same readiness, first. Then the assimilation parameters and the observation preprocessing will also need to be refined and investigated to extract the most from e-profile and VIIRS observations. One limitation of both instruments is the fact they provide an information on aerosols with no indication on the species. More advanced information, such as specific dust AOD, could be very useful to enhance the impact of aerosol observations in the regional systems.

6 References

Badia, A., Jorba, O., Voulgarakis, A., Dabdub, D., Pérez García-Pando, C., Hilboll, A., Gonçalves, M., and Janjic, Z.: Description and evaluation of the Multiscale Online Nonhydrostatic AtmospheRe CHemistry model (NMMB-MONARCH) version 1.0: gas-phase chemistry at global scale, Geosci. Model Dev., 10, 609–638, https://doi.org/10.5194/gmd-10-609-2017, 2017.

Colette, Augustin and Collin, Gaëlle and Besson, François and Blot, Etienne and Guidard, Vincent and Meleux, Frederik and Royer, Adrien and Petiot, Valentin and Miller, Claire and Fermond, Oihana and others. (2024). Copernicus Atmosphere Monitoring Service–Regional Air Quality Production System v1. 0. EGUsphere, 2024:1–92.

Desroziers, G., Berre, L., Chapnik, B., and Poli, P. (2005). Diagnosis of observation, background and analysis-error statistics in observation space. Quarterly Journal of the Royal Meteorological Society, 131(613):3385–3396.

Di Tomaso, E., Escribano, J., Basart, S., Ginoux, P., Macchia, F., Barnaba, F., Benincasa, F., Bretonnière, P.-A., Buñuel, A., Castrillo, M., Cuevas, E., Formenti, P., Gonçalves, M., Jorba, O., Klose, M., Mona, L., Montané Pinto, G., Mytilinaios, M., Obiso, V., Olid, M., Schutgens, N., Votsis, A., Werner, E., and Pérez García-Pando, C.: The MONARCH high-resolution reanalysis of desert dust aerosol over Northern Africa, the Middle East and Europe (2007–2016), Earth Syst. Sci. Data, 14, 2785–2816, https://doi.org/10.5194/essd-14-2785-2022, 2022.

El Amraoui, Laaziz and Plu, Matthieu and Guidard, Vincent and Cornut, Flavien and Bacles, Mickaël. (2022). A pre- operational system based on the assimilation of MODIS aerosol optical depth in the MOCAGE chemical transport model. Remote Sensing, 14(8):1949.

Guth, Jonathan and Josse, Béatrice and Marécal, Virginie and Joly, M and Hamer, P. (2016). First implementation of secondary inorganic aerosols in the MOCAGE version R2. 15.0 chemistry transport model. Geoscientific Model Development, 9(1), 137–160.

Haustein, K., Pérez, C., Baldasano, J. M., Jorba, O., Basart, S., Miller, R. L., Janjic, Z., Black, T., Nickovic, S., Todd, M. C., Washington, R., Müller, D., Tesche, M., Weinzierl, B., Esselborn, M., and Schladitz, A.: Atmospheric dust modeling from meso to global scales with the online NMMB/BSC-Dust model – Part 2: Experimental campaigns in Northern Africa, Atmos. Chem. Phys., 12, 2933–2958, https://doi.org/10.5194/acp-12-2933-2012, 2012.

Janjic, Z. and Gall, L.: Scientific documentation of the NCEP nonhydrostatic multiscale model on the B grid (NMMB), Part 1 Dynamics, NCAR/TN-489+STR, https://doi.org/10.5065/D6WH2MZX, 2012.

Jorba, O., Dabdub, D., Blaszczak-Boxe, C., Pérez, C., Janjic, Z., Baldasano, J., Spada, M., Badia, A., and Gonçalves, M.: Potential significance of photoexcited NO2 on global air quality with the NMMB/BSC chemical transport model, J. Geophys. Res.-Atmos., 117, https://doi.org/10.1029/2012JD017730, 2012.

Klose, M., Jorba, O., Gonçalves Ageitos, M., Escribano, J., Dawson, M. L., Obiso, V., Di Tomaso, E., Basart, S., Montané Pinto, G., Macchia, F., Ginoux, P., Guerschman, J., Prigent, C., Huang, Y., Kok, J. F., Miller, R. L., and Pérez García-Pando, C.: Mineral dust cycle in the Multiscale Online Nonhydrostatic AtmospheRe CHemistry model (MONARCH) Version 2.0, Geosci. Model Dev., 14, 6403–6444, https://doi.org/10.5194/gmd-14-6403-2021, 2021a.

Parrish, David F and Derber, John C. (1992). The National Meteorological Center's spectral statistical-interpolation analysis system. Monthly Weather Review, 120(8):1747–1763.

Pérez, C., Haustein, K., Janjic, Z., Jorba, O., Huneeus, N., Baldasano, J. M., Black, T., Basart, S., Nickovic, S., Miller, R. L., Perlwitz, J. P., Schulz, M., and Thomson, M.: Atmospheric dust modeling from meso to global scales with the online NMMB/BSC-Dust model – Part 1: Model

description, annual simulations and evaluation, Atmos. Chem. Phys., 11, 13001–13027, https://doi.org/10.5194/acp-11-13001-2011, 2011.

Spada, M., Jorba, O., Pérez García-Pando, C., Janjic, Z., and Baldasano, J. M.: Modeling and evaluation of the global sea-salt aerosol distribution: sensitivity to size-resolved and sea-surface temperature dependent emission schemes, Atmos. Chem. Phys., 13, 11735–11755, https://doi.org/10.5194/acp-13-11735-2013, 2013.

Document History

Version	Author(s)	Date	Changes
1.0	V Guidard, G Monteil, A Uppstu	28 november 2025	Initial version
1.1	V Guidard	18 December 2025	Taking minor comments into account

Internal Review History

Internal Reviewers	Date	Comments
A Lipponen	10 December 2025	Minor comments added.
C. Granier	16 December 2025	Minor comments added